JOURNAL OF OPTOELECTRONICS AND ADVANCED MATERIALS Vol. 16, No. 5-6, May - June 2014, p. 591 - 599

Evaluation of noise parameter characterization methods for radio frequency integrated circuit (RFIC) device

S. KORAKKOTTIL KUNHI MOHD[a,b*], NORLAILI MOHD NOH[b], O. SIDEK[a]
[a]*Collaborative Microelectronic Design Excellence Centre, Universiti Sains Malaysia, Pulau Pinang, Malaysia*
[b]*School of Electrical and Electronic Engineering, Universiti Sains Malaysia, Pulau Pinang, Malaysia*

This study evaluates several tuner-less noise parameter characterization methods. The theory, equation, and procedure are described in detail as implemented in this study. The tuner-less noise parameter characterization methods are classified into three categories: noise power, direct, and multiple source impedance methods. Comparison of the conventional noise parameter characterization method with the three categories is performed in terms of the measurement setup and procedure. The advantage of each method over the other is also highlighted. The objective of this work is to provide an overview in choosing the best method for the noise characterization based on available resources. In addition, from the comprehensive theory, equation, and procedure as given in this paper, an in-depth knowledge about the accurate tuner-less noise characterization methods can be acquired.

(Received July 25, 2013; accepted May 15, 2014)

Keywords: Noise characterization, Noise parameter, Tuner-less noise parameter, Noise extraction, Review on noise measurement

1. Introduction

The noise performance of a receiver in a wireless communication system largely depends on the low-noise amplifier (LNA), as LNA is the first component in the receiver path [1]. The remarkable progress in the recent device technology creates a strong demand for accurate noise characterization [2]. To achieve the objective, determination of four noise parameters is required, which are deduced from noise figure (NF) behavior with variations of source impedance (Z_S), source admittance (Y_S), or source reflection coefficient (Γ_S). These variations are usually accomplished using a tuner. NF is measured for each of these variations in order to acquire several noise equations, where by solving these equations yield the noise parameter [3]. At least four NF measured at different Z_S, Y_S, or Γ_S are required to extract all the four noise parameters. However, more than four measurements are usually performed to improve the accuracy and for averaging purposes [4]. The implementation of this method actually suffers from a few constraints due to high cost of the tuner, complicated setup and procedure, time-consuming calibration, and long measurement period, which motivate researchers to explore an alternative methods for the noise parameter characterization [5].

Several groups have presented their respective approaches to characterize the noise parameter over time. The methods can be summarized into three: noise parameter characterization based on the noise power, direct approach, and multiple source impedance methods. For the noise power method, a signal flow diagram is required to represent the whole measurement setup. The signal flow diagram is drawn in accordance to the signal waves that flow through out the setup. In the noise power method, the available noise power is measured together and without a device under test (DUT) [6,7]. Then, several equations are derived from the signal flow diagram and the noise power measurement. This will finally lead to the noise parameter [8,9]. The second category involves the direct approach for noise parameter characterization by calculating the noise parameter directly from noise correlation matrix [10,11]. This method requires S-parameter and NF data measured on the basis of the system impedance for the instruments used, where the commonly known system impedance for the radio frequency integrated circuit (RFIC) is 50 Ω [5,12-15]. No variation to the source condition is required. Small signal and noise equivalent model that describes the noise behavior of the DUT is utilized [16,17]. The third category of noise parameter characterization is based on multiple source impedance, where it is almost similar to the tuner-based extraction system except for the absence of tuner [3,18,19]. The multiple source impedance method relies on the principle of producing several noise equations, which are obtained from the NF measurement performed under different source conditions [20-23]. However, instead of using a tuner, other mechanisms that can alter and vary the source conditions are implemented. The data produced are usually compressed to a minimum because the number of different Z_S, Y_S, and Γ_S generated is not equal to that using the tuner but is adequate for the extraction of the noise parameter.

This study evaluates all the three tuner-less noise parameter characterization methods from the perspectives of the theory, equation, and procedure. The motivations for this review is to collect, evaluate, and compare the three categories with the conventional method. This study will also provide an overview on which method would be

suitable for certain measurement conditions assuming that all methods produce accurate results. This paper is organized as follows: Section II gives an overview of general noise parameter characterization. Section III discusses detailed procedure for all the three categories. Section IV discusses on the advantage and disadvantage of the three methods and finally, Section V presents the summary and conclusion. Additionally, appendix is given in Section VI.

2. Principle of noise parameter characterization

The general noise parameter characterization setup is shown in Fig. 1. Theoretically, NF is known as the parameter that characterizes the ability of a device to process a low-level signal [24]. On the other hand, the noise parameter explains how NF varies with Z_S, Y_S, and Γ_S. Various equations of noise parameter exist, and they are formulated in (1)-(4) [25]. NF is the numerical ratio of the noise factor (F), where NF is expressed in decibels.

$$F = F_{\min} + \frac{4R_n}{Z_o}\frac{\left|\Gamma_S - \Gamma_{opt}\right|^2}{\left(1-\left|\Gamma_S\right|^2\right)\left|1+\Gamma_{opt}\right|^2}, \quad (1)$$

The four noise parameters are the following:
R_n: equivalent noise resistance
F_{min}: minimum NF (measured at Γ_{opt})
$|\Gamma_{opt}|$: magnitude of the optimum noise reflection
$\angle\Gamma_{opt}$: phase of the optimum noise reflection
$\Gamma_{opt} = |\Gamma_{opt}|\angle\Gamma_{opt}$

$$F = F_{\min} + \frac{G_n}{R_S}\left[\left|Z_S - Z_{opt}\right|^2\right], \quad (2)$$

The four noise parameters are the following:
G_n: equivalent noise conductance
F_{min}: minimum NF (measured at Z_{opt})
R_{opt}: optimum noise resistance
X_{opt}: optimum noise reactance
$Z_{opt} = R_{opt} + jX_{opt}$

$$F = F_{\min} + \frac{N}{\mathrm{Re}(Y_{opt})}\frac{\left|Z_S - Z_{opt}\right|^2}{\mathrm{Re}(Y_S)}, \quad (3)$$

The four noise parameters are the following:
N: terminal invariant constant
F_{min}: minimum NF (measured at Y_{opt})
G_{opt}: optimum conductance
B_{opt}: optimum susceptance
$Y_{opt} = G_{opt} + jB_{opt}$

$$N = \left[F\left(Y_{opt}\right) - F_{\min}\right]\frac{1-\left|\Gamma_{opt}\right|^2}{4\left|\Gamma_{opt}\right|^2}$$

and,

$$F = F_{\min} + \frac{R_n}{G_S}\left[\left(G_S - G_{opt}\right)^2 + \left(B_S - B_{opt}\right)^2\right]. \quad (4)$$

The four noise parameters are the following:
R_n: equivalent noise resistance
F_{min}: minimum NF (measured at Y_{opt})
G_{opt}: optimum conductance
B_{opt}: optimum susceptance
$Y_{opt} = G_{opt} + jB_{opt}$

One common parameter in all the equations is F_{min}, which can be achieved at the specific point of either Z_{opt}, Y_{opt}, or Γ_{opt}. R_n, G_n, and N are the scale factors.

Basically from these equations, by introducing a minimum of four Z_S, Y_S, or Γ_S at the input stage, four noise equations can be obtained. The noise parameter is achieved by resolving the unknown in the equations. To improve the accuracy, more than four Z_S, Y_S, or Γ_S are usually introduced at the input stage, which will create more equations. Then, the method of least square fit is applied to extract the noise parameter. In general, noise parameter measurement setup is as shown in Fig. 1. The vector network analyzer (VNA) and NF analyzer (NFA) are used for the S-parameter and NF measurements, respectively. The semiconductor parameter analyzer provides voltage supply while simultaneously monitoring current consumed by the DUT. The switches in the setup are used to select between the S-parameter and the NF measurements. The square with the dotted line represents the accessory used to vary the conditions of the input stage. Z_S, Y_S, and Γ_S are related to one another; thus, changes in one of these values will affect the others. For the extraction methods (refer to Appendix 6.1), the least square method is generally applied [26].

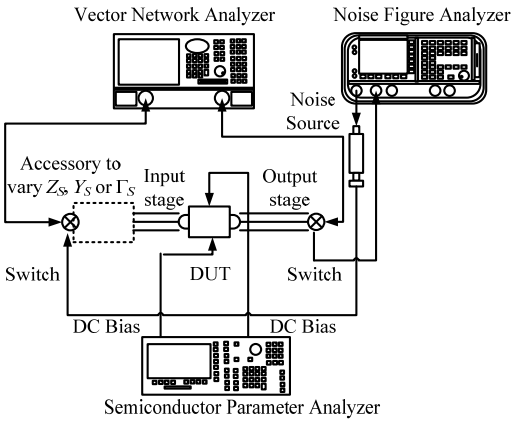

Fig. 1. General noise parameter characterization setup.

3. Noise parameter characterization

Aside from using a tuner, various groups have developed a tuner-less method for noise parameter characterization. The tuner-less method is categorized into three: noise power, direct, and multiple source impedance methods.

3.1 Noise power method

The noise power method relies on the equations derived from signal flow diagram. The setup is almost similar to that shown in Fig. 1, however, the accessory at the input stage is load impedance. Complete setup for the noise power method is shown in Fig. 2. The setup is divided into three reference planes: P1, P2, and P3. P1 and P2 represent the reference plane at the interconnections between input and output stages with the DUT. P3 is the reference plane at the interconnection between the input stage and the load impedance. Signal flow diagram of the setup is as shown in Fig. 3. Following steps below described the characterization procedure for noise power method.

Step 1: For calibration, the connection shown in Fig. 2, is performed. However, the DUT is removed and replaced with a 'THROUGH' standard. The 'THROUGH' standard ensures direct interconnection between the input and output stages. Therefore, the space between planes P1 and P2 in Fig. 3 can be removed. Using the non-touching loop rule (refer to Appendix 6.2), the power wave equation b seen from the NFA is derived as [8],

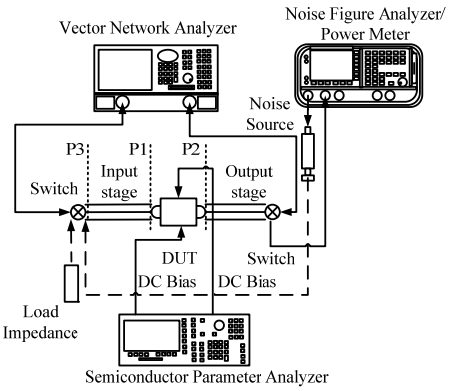

Fig. 2. Noise parameter characterization based on the noise power method.

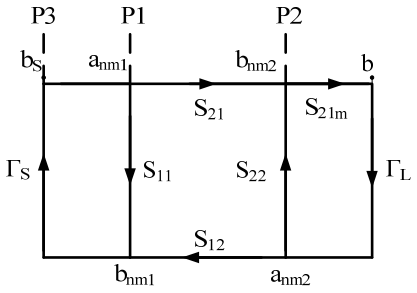

Fig. 3. Signal flow diagram for the noise parameter characterization based on the noise power method.

$$b = \frac{b_S b_{21m}}{1-\Gamma_S\Gamma_L} + \frac{b_{nm1}\Gamma_S\Gamma_L}{1-\Gamma_S\Gamma_L} + b_{nm2}\ , \tag{5}$$

where the power obtained from NFA is defined as [8],

$$N = \langle b.b^* \rangle\ . \tag{6}$$

Therefore [8],

$$\begin{aligned} N = {} & kT_S\Delta f\left(1-|\Gamma_S|^2\right)\frac{|S_{21m}|^2}{|1-\Gamma_S\Gamma_L|^2} \\ & + \left\langle b_{nm1}\cdot b^*_{nm1}\right\rangle |S_{21m}|^2\frac{|\Gamma_S|^2}{|1-\Gamma_S\Gamma_L|^2} \\ & + \left\langle b_{nm1}\cdot b^*_{nm2}\right\rangle \\ & + 2\,\mathrm{Re}\left(\left\langle b_{nm1}\cdot b^*_{nm2}\right\rangle S_{21m}\right)\mathrm{Re}\left(\frac{\Gamma_S}{1-\Gamma_S\Gamma_L}\right) \\ & - 2\,\mathrm{Im}\left(\left\langle b_{nm1}\cdot b^*_{nm2}\right\rangle S_{21m}\right)\mathrm{Im}\left(\frac{\Gamma_S}{1-\Gamma_S\Gamma_L}\right) \end{aligned}\ . \tag{7}$$

T_S is the source temperature. To solve the unknowns in (7), i.e., $k\Delta f|S_{21m}|^2$, $\langle b_{nm1}.b^*_{nm1}\rangle|S_{21m}|^2$, $\langle b_{nm2}.b^*_{nm2}\rangle$, $\mathrm{Re}(\langle b_{nm1}.b^*_{nm2}\rangle\ S_{21m})$, and $I_m(\langle b_{nm1}.b^*_{nm2}\rangle\ S_{21m})$, five equations are required [9].

$$\begin{pmatrix} N_1 \\ N_2 \\ N_3 \\ N_4 \\ N_5 \end{pmatrix} = (M_m)\begin{pmatrix} k\Delta f|S_{21m}|^2 \\ \langle b_{nm1}\cdot b^*_{nm1}\rangle|S_{21m}|^2 \\ \langle b_{nm2}\cdot b^*_{nm2}\rangle \\ \mathrm{Re}\left(\langle b_{nm1}\cdot b^*_{nm2}\rangle S_{21m}\right) \\ \mathrm{Im}\left(\langle b_{nm1}\cdot b^*_{nm2}\rangle S_{21m}\right) \end{pmatrix} = (M_m)\begin{pmatrix} X_1 \\ X_2 \\ X_3 \\ X_4 \\ X_5 \end{pmatrix}, \tag{8}$$

where

$$\begin{aligned} M_{m1} &= T_{1S}\frac{\left(1-|\Gamma_{1S}|^2\right)}{|1-\Gamma_{1S}\Gamma_{1L}|^2} \\ M_{m2} &= \frac{|\Gamma_{2S}|^2}{|1-\Gamma_{2S}\Gamma_{2L}|^2} \\ M_{m3} &= 1 \\ M_{m4} &= 2\,\mathrm{Re}\left(\frac{\Gamma_{4S}}{1-\Gamma_{4S}\Gamma_{4L}}\right) \\ M_{m5} &= -2\,\mathrm{Im}\left(\frac{\Gamma_{5S}}{1-\Gamma_{5S}\Gamma_{5L}}\right) \end{aligned}\ , \tag{9}$$

m1 to *m5* represent the different Γ_S introduced. N_1 to N_5 are the noise power measured under different Γ_S. Γ_{1S} to Γ_{5S} are the first to fifth Γ_S, whereas Γ_{1L} to Γ_{5L} are the first to fifth Γ_L. Γ_L is the load reflection coefficient, where it is usually measured at the output stage.

Step 2: For Γ_{1S}, the noise source is connected to the switch. The noise source is turned 'ON' and Γ_{1S} and Γ_{1L} are measured to solve (8).

Step 3: For the second to fifth conditions of Γ_S and Γ_L, the noise source is replaced with the load impedance ('OPEN', 'SHORT', 'OPEN' attenuator, 'SHORT' attenuator). Step 2 is repeated for the second to the fifth

conditions of Γ_S. Based on (7), (8) and (1), the following equation is derive [8],

$$F_m = 1+ \frac{\dfrac{X_2\left|\Gamma_S\right|^2}{\left|1-\Gamma_S\Gamma_L\right|^2} + X_3 + 2\,\mathrm{Re}\left(\left(X_4+jX_5\right)\dfrac{\Gamma_s}{1-\Gamma_S\Gamma_L}\right)}{X_2T_o\dfrac{1-\left|\Gamma_S\right|^2}{\left|1-\Gamma_S\Gamma_L\right|^2}} \quad (10)$$

where F_m represents the NF during the calibration. Comparing (10) and (1) yields [8],

$$\Gamma_{mopt} = \frac{A_m + C_m - \sqrt{\left(A_m+C_m\right)^2 - 4\left|B_m\right|^2}}{2\left|B_m\right|}$$

$$R_{mn} = \frac{\left|B_m\right|\left|1+\Gamma_{mopt}\right|^2}{4\left|\Gamma_{mopt}\right|} \quad (11)$$

$$F_{m\min} = C_m - \frac{4R_{mn}\left|\Gamma_{mopt}\right|^2}{\left|1+\Gamma_{mopt}\right|^2}$$

where

$$A_m = -1 + \frac{X_2}{X_1T_o} + \frac{X_3\left|\Gamma_L\right|^2}{X_1T_o} - \frac{\left(X_4+jX_5\right)\Gamma_L^*}{X_1T_o} - \frac{\left(X_4+jX_5\right)\Gamma_L}{X_1T_o}$$

$$B_m = -X_3\frac{\Gamma_L}{X_1T_o} + \frac{\left(X_4+jX_5\right)}{X_1T_o} \quad (12)$$

$$C_m = 1 + \frac{X_3}{X_1T_o}$$

Once (12) is resolved, noise parameter of the bench can be obtained using (11).

Step 4: The 'THROUGH' standards are replaced with the DUT. Steps 1–3 are repeated to obtain the noise parameter of the DUT and the bench. Using the data from calibration procedure enables extraction of the DUT noise parameters.

The above method assumes that the effects of the input and output stages are subtracted before the measurement is done. This requires another complicated technique. In [6] and [7], the authors proposed a different approach to subtract the input and output stage effects by including them in the derivation of the signal flow diagram. The effects of the input and output stages are defined as attenuation α and electrical delay, τ. Then, instead of using the extraction method described in (10), (11) and (12), they used the time-domain approach by solving α and τ in the noise equation.

3.2 Direct method

Gao et al. introduced the direct noise parameter measurement that involves knowledge of the small signal equivalent circuit and the noise correlation matrix of the DUT [16], [17]. For case study, all noise sources from the equivalent circuit model, which is pseudormorphic high electron-mobility transistors (pHEMT) are identified and equations for the noise parameter are developed as,

$$\begin{aligned} F'_{\min} &= 1 + K_B\omega \\ G'_{opt} &= K_C\omega \\ B'_{opt} &= K_D\omega \\ R'_n &= K_E \end{aligned} \quad . \quad (13)$$

K_B, K_C, K_D, and K_E are the fitting factors used for iteration purposes, whereas F'_{min}, G'_{opt}, B'_{opt}, and R'_n are the initial noise parameters, which are utilized during the iterative calculations to extract the actual noise parameters. ω is the angular frequency. These fitting factors can be determined from the NF equation in the 50-Ω system impedance, expressed as

$$F_{50} = 1 + R_nG_o + \frac{R_n}{G_o}\left|Y_{opt}\right|^2 . \quad (14)$$

R'_n in (14) is frequency independent, in contrast to frequency-dependent Y_{opt}. Therefore, at $\omega = 0$, (14) can be written as,

$$F_{50}^{\omega=0} = 1 + R_nG_o , \quad (15)$$

where $G_o = 20mS$ at 50-Ω system impedance. Once R'_n is known, Y_{opt} can be determined from

$$F_{\min} = 1 + 2R_nG_{opt} . \quad (16)$$

The initial noise parameter from (14), (15) and (16) are substituted to (13). NF is calculated based on the fitting factors and noise correlation matrix. At the same time, the NF of the DUT is measured, and the difference between the calculation and measurement is noted. The fitting factors are updated accordingly until the difference is not too large.

3.3 Noise parameter characterization based on multiple source impedance method

The multiple source impedance method relies on assumption that the NF result is dependent on the input impedance. From (1) to (4), the changes in the input impedance lead to several NF equations with the noise parameter as the unknown. Certain approaches are available to vary the input impedance, and generally, a tuner is used.

Tiemeijer et al. proposed different solutions instead of using a tuner [19]. Their method incorporated a coupler to

interconnect between the measurement system and three selectable impedance standards, as shown in Fig. 4. In addition, they also improved the currently available NF measurement technique, which is based on the *y*-factor method (refer to Appendix 6.3). Reason for the improvement is that the noise source admittance is not necessarily the same for the 'HOT' and 'COLD' states. 'HOT' refers to the case when the noise source is turned 'ON', whereas 'COLD' refers to that when the noise source is turned 'OFF'. Therefore, the NF measurement for the noise parameter characterization must be corrected so that difference between the 'HOT' and 'COLD' admittances can be eliminated. The method starts by first, adopting the *y*-factor equation [19],

$$Y = \frac{kT_o BG_H \left(F_H - 1\right) + kT_H BG_H}{kT_o BG_C \left(F_C - 1\right) + kT_C BG_C} \ . \tag{17}$$

where G_H, G_C, T_H, and T_C are the gain and temperature measured during the 'HOT' and 'COLD' states, respectively. The effective *y*-factor *(Y')*, used to incorporate changes in the device gain during the 'HOT' and 'COLD' states from (17) can be written as [19],

$$Y^{'} = Y\frac{G_C}{G_H} = \frac{F_H + \dfrac{T_H - T_o}{T_o}}{F_C + \dfrac{T_C - T_o}{T_o}} \ , \tag{18}$$

Equation (18) is then rearranged to [19],

$$Y^{'}F_C - F_H = \frac{T_H - T_o}{T_o} - Y^{'}\left(\frac{T_C - T_o}{T_o}\right) , \tag{19}$$

where,

$$ENR^{'} = \frac{T_H - T_o}{T_o} - Y^{''}\left(\frac{T_C - T_o}{T_o}\right) , \tag{20}$$

'ENR`' is the effective excess noise ratio (ENR) that includes the effect of admittance changes between the 'HOT' and 'COLD' states. Based on (40) and (19), when (20) is substituted into (4), the NF equation becomes [19],

$$F_{C,H} = \frac{ENR^{'}}{Y^{'} - 1} = F_{\min} + R_n\left[\frac{Y^{'}}{Y^{'} - 1}\frac{\left|Y_C - Y_{opt}\right|^2}{\mathrm{Re}\left(Y_C\right)} - \frac{1}{Y^{'} - 1}\frac{\left|Y_C - Y_{opt}\right|^2}{\mathrm{Re}\left(Y_C\right)}\right] , \tag{21}$$

where Y_C, Y_H, and Y_{opt}, are the source admittance at the 'COLD', 'HOT', and optimum states, respectively. To resolve the noise parameter, (21) is linearized by variable substitution [19],

$$F = a_1 x_1 + a_2 x_2 + a_3 x_3 + a_4 x_4 \ , \tag{22}$$

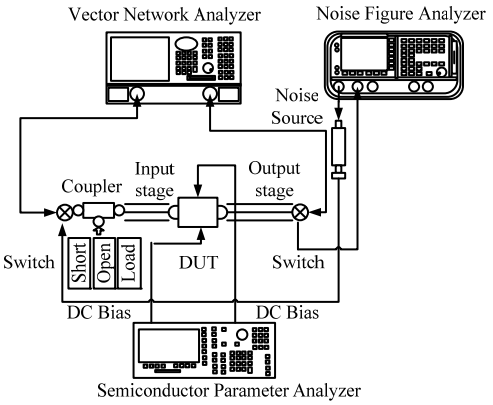

Fig. 4. Noise parameter characterization system for the multiple source impedance method.

where, using partial fraction,

$$\begin{aligned} a_1 &= \frac{Y^{'}}{Y^{'} - 1}\frac{\left|Y_C\right|^2}{\mathrm{Re}\left(Y_C\right)} + \frac{-1}{Y^{'} - 1}\frac{\left|Y_H\right|^2}{\mathrm{Re}\left(Y_H\right)} \\ a_2 &= \frac{2Y^{'}}{Y^{'} - 1}\frac{\mathrm{Im}\left(Y_C\right)}{\mathrm{Re}\left(Y_C\right)} + \frac{2}{Y^{'} - 1}\frac{\mathrm{Im}\left(Y_H\right)}{\mathrm{Re}\left(Y_H\right)} \\ a_3 &= \frac{Y^{'}}{Y^{'} - 1}\frac{1}{\mathrm{Re}\left(Y_C\right)} + \frac{-1}{Y^{'} - 1}\frac{1}{\mathrm{Re}\left(Y_H\right)} \\ a_4 &= 1 \end{aligned} \ . \tag{23}$$

The partial fraction is obtained by assuming that

$$\begin{aligned} x_1 &= R_n \\ x_2 &= \mathrm{Im}\left(Y_{opt}\right)R_n \\ x_3 &= \mathrm{Re}\left(Y_{opt}\right)^2 R_n \\ x_4 &= F_{\min} - 2\,\mathrm{Re}\left(Y_{opt}\right)R_n \end{aligned} \ . \tag{24}$$

Equation (24), which yields the noise parameter, is resolved by having several data sets from (22).

The first step in this method is to measure Y_H, Y_C, T_C, Y, NF, G_H, and G_C. These parameters must be measured under three impedance standards, namely, 'OPEN,' 'SHORT,' and 'LOAD' and under three closely spaced adjacent frequencies. The procedure is performed based on the assumption that the reflection coefficient and NF will vary proportionally and accordingly under the three closely spaced adjacent frequencies.

Y_H, Y_C, G_H, and G_C can be obtained by measuring the S-parameter of the input and output stages, together with the S-parameter of the DUT. The measurement setup for both the input and output stages are shown in Fig. 5. Because both input and output stages consist of asymmetrical connector ends, the one-port S-parameter measurement must be employed, where the procedures are discussed in [27]. The one-port S-parameter measurement must be done for three impedance standards and under three adjacent frequencies. The NFA and noise source are included in the setup to create the 'HOT' and 'COLD' states, as shown in Fig. 5. From the S-parameter of the

input stage, the source admittance can be obtained using [28],

$$Y_H / Y_C = \frac{(1+S_{22})(1-S_{11})+S_{12}S_{21}}{(1+S_{11})(1-S_{22})+S_{12}S_{21}} \quad . \tag{25}$$

NF is measured using the measurement setup shown in Fig. 4, whereas the *Y*-factor can be obtained from [29],

$$Y = \frac{F+ENR}{F+\dfrac{T_C - T_o}{T_o}} \quad . \tag{26}$$

T_C in (19) is measured by connecting the noise source directly to the NFA, as shown in Fig. 6.

In addition to the impedance standard, the variation in the input impedance can be realized using a phase shifter [3]. The phase shifter alters the phase of the propagating signal at the input stage, thus changing Z_S, Y_S, or Γ_S. The phase shifter design was proposed by Gu et al. and is shown in Fig. 7 [3]. The phase shifter designed almost similar to the coupler. However, the isolated port is terminated at the OPEN state. A varactor is added to tune the capacitor values, which then provide the phase difference. The phase shifter designed by Gu et al. was fabricated on a printed circuit board (PCB) and has a small footprint. Another method of varying the input impedance was proposed by Hu et al., which utilized a mismatched circuit that provided the impedance difference [30].

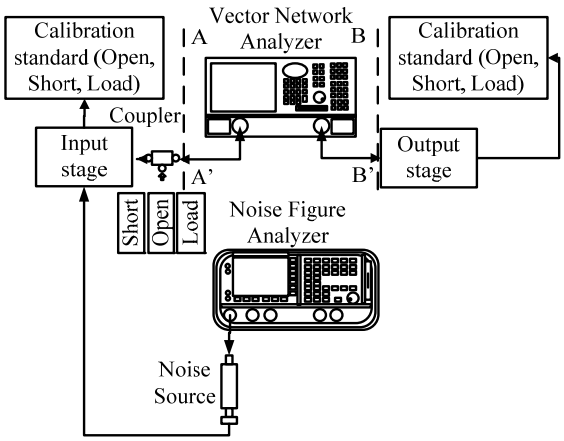

Fig. 5. Measurement setup for both the input and output stages.

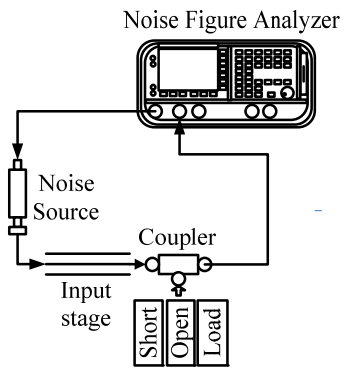

Fig. 6. Measurement setup for T_C in three impedance standards and under three closely spaced frequencies.

The mismatched circuit can be fabricated on the PCB and has a small footprint.

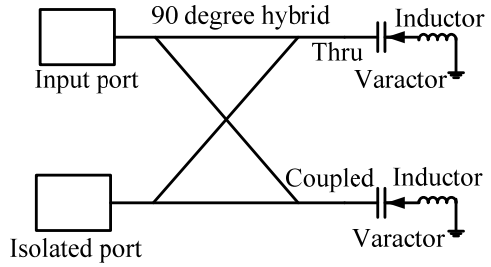

Fig. 7. Schematic of phase shifter for noise parameter measurement.

4. Discussion

The first category of noise parameter characterization does not require any NF measurement, in contras to the second and third categories. Only the power measurement is involved. Basically, two methods are available to perform the NF measurement, which are known as the 'COLD' and *y*-factor measurements. 'COLD' is a passive measurement, where the noise source is turned 'OFF' during the operation. The *y*-factor measurement is a combination of the 'HOT' and 'COLD'. The noise source produces a thermal noise during the 'COLD' state and a large amount of noise during the 'HOT' state. Most literature claims that the 'COLD' measurement is more accurate than the *y*-factor measurement because in the 'COLD' measurement, the admittance of the source is standardized throughout the measurement and will not jeopardize the result. However, Tiemeijer et al. has shown that the changes in the admittance for the *y*-factor method can be corrected [19]. Depending on one's convenience, both methods can be used.

The measurement setup for all the three categories adopts almost similar setup as shown in Fig. 1, except for the use of different accessories at the input stage.

4.1 Noise parameter characterization based on the noise power method

The advantage of the noise power method over the others is that the noise performance of the DUT can be measured without using the NFA. This method requires only a power measurement where the spectrum analyzer or PM can be used instead of the NFA. The result is almost identical to the expected result. Although ripples are visible on the result, averaging can solve the problem. The only external knowledge required to perform the measurement using the noise power method is the non-touching loop rule, which is explained briefly in Appendix 6.2. The non-touching loop rule is needed to derive the noise equations from the signal flow diagram. The setup for the noise power method utilizes noise source and four load impedances as an accessory to vary the source impedance. The noise source can be operated independently without the NFA, where it can be turned on using a normal power supply.

4.2 Noise parameter characterization based on direct method

The direct method only requires a general NF measurement. However, it needs the knowledge of the small signal equivalent circuit model to derive a set of expressions for the noise parameter in (13). These expressions are different, depending on the chosen model. Therefore, before starts the measurement, all the noise sources of the DUT must be listed according to the equivalent circuit so that the expression of the noise parameter can be derived. In terms of the measurement results, the direct measurement method yields smoother results compared with the noise power method. This method does not need any other accessory to be included in the measurement setup, as shown in Fig. 1.

4.3 Noise parameter characterization based on multiple source impedance method

The multiple source impedance is almost similar to the conventional method except that tuner is replaced with typical impedance standards. These impedance standards minimize the amount of NF measurement, resulting simpler extraction. Even though the method described in this paper requires nine sets of equations, another study proved that four equations are adequate [18]. The only constraint in making the measurement using this method is in understanding the extraction part, which requires strong mathematical skills.

5. Conclusions

We have reviewed the noise parameter characterization methods where the tuner-less procedure was focused. The reviewed methods were divided into three categories: noise power, direct, and multiple source impedance methods. For the noise power method, no noise measurement is involved, which makes it perfect when NFA is not available. The direct method requires derivation of a small signal noise equivalent model in order to acquire sets of noise expression, and no variation in the source condition is required. Finally, the multiple source impedance method employs an almost similar procedure as that of the tuner-based method. The only difference is that the number of different source impedance introduced at the input stage is compressed to a minimum but is adequate for noise parameter extraction.

6. Appendix

6.1 Least squares method

Least squares method gives the minimum sum of the square deviations from the measured values using the approximation curve $y = f(x)$ [26].

$$E = \sum_{i=1}^{n} \left| y_i - f\left(x_i\right) \right|^2 = \min \ , \tag{27}$$

where y_i is set of measured data. Equation (4) is rearranged to,

$$F = F_{\min} - 2R_n G_{opt} + \frac{G_S^2 + B_S^2}{G_S} + \frac{1}{G_S} R_n \left(G_{opt}^2 + B_{opt}^2\right) - \frac{B_S}{G_S} 2R_n B_{opt} \ . \tag{28}$$

Then, the following substitutions are employed:

$$\begin{aligned} A &= F_{\min} - 2R_n G_{opt} \\ B &= R_n \\ C &= R_n \left(G_{opt}^2 + B_{opt}^2\right) \\ D &= -2R_n B_{opt} \end{aligned} \ , \tag{29}$$

where:

$$\begin{aligned} F_{\min} &= A + 4BC - D2 \\ R_n &= B \\ G_{opt} &= \frac{4BC - D^2}{2B} \\ B_{opt} &= -\frac{D}{2B} \end{aligned} \ . \tag{30}$$

Equation (29) gives a linearized function to (28) and yields,

$$\begin{aligned} F &= A + \left(G_S + \frac{B_S^2}{G_S} \right) B + \frac{1}{G_S} C + \frac{B_S}{G_S} D, \\ F_i &= f\left(G_{Si}, B_{Si}, A, B, C, D\right) \end{aligned} \ . \tag{31}$$

i is the number of NF measurements with different Z_S, Y_S, or Γ_S. By obtaining the partial derivatives of (31),

$$\begin{aligned} &\frac{\partial F}{\partial A} = 1, \frac{\partial F}{\partial B} = G_S + \frac{B_S^2}{G_S}, \frac{\partial F}{\partial C} = \frac{1}{G_S}, \frac{\partial F}{\partial D} = \frac{B_S}{G_S} \\ &\left(\frac{\partial F}{\partial A}\right)_i = 1, \left(\frac{\partial F}{\partial B}\right)_i = G_{Si} + \frac{B_{Si}^2}{G_{Si}}, \\ &\left(\frac{\partial F}{\partial C}\right)_i = \frac{1}{G_{Si}}, \left(\frac{\partial F}{\partial D}\right)_i = \frac{B_{Si}}{G_{Si}} \end{aligned} \ . \tag{32}$$

Applying (27) to (31) and (32) yields,

$$\begin{aligned} &\sum_{i=1}^{n} \left[F_i - A - \left(G_{Si} + \frac{B_{Si}^2}{G_{Si}} \right) B - \frac{1}{G_{Si}} C - \frac{B_{Si}}{G_{Si}} D \right] = 0, \\ &\sum_{i=1}^{n} \left[F_i - A - \left(G_{Si} + \frac{B_{Si}^2}{G_{Si}} \right) B - \frac{1}{G_{Si}} C - \frac{B_{Si}}{G_{Si}} D \right] \left(G_{Si} + \frac{B_{Si}^2}{G_{Si}} \right) = 0, \\ &\sum_{i=1}^{n} \left[F_i - A - \left(G_{Si} + \frac{B_{Si}^2}{G_{Si}} \right) B - \frac{1}{G_{Si}} C - \frac{B_{Si}}{G_{Si}} D \right] \frac{1}{G_{Si}} = 0, \\ &\sum_{i=1}^{n} \left[F_i - A - \left(G_{Si} + \frac{B_{Si}^2}{G_{Si}} \right) B - \frac{1}{G_{Si}} C - \frac{B_{Si}}{G_{Si}} D \right] \frac{B_{Si}}{G_{Si}} = 0 \end{aligned} \tag{33}$$

Further modification yields a set of four linearized equations, i.e.,

$$\begin{aligned} A.A_{11} + B.A_{12} + C.A_{13} + D.A_{14} &= A_{15} \\ A.A_{21} + B.A_{22} + C.A_{23} + D.A_{24} &= A_{25} \\ A.A_{31} + B.A_{32} + C.A_{33} + D.A_{34} &= A_{35} \\ A.A_{41} + B.A_{42} + C.A_{43} + D.A_{44} &= A_{45} \end{aligned} \quad . \tag{34}$$

Because A_{11} to A_{45} are the same, the (35) can be used to solve (34). Substitution of the A, B, C, and D results from (31) to (34) lead to the noise parameter data.

6.2 Non-touching loop rule

The non-touching loop rule provides solution to derive an equation from the signal flow graph. The solution

$$\begin{aligned} &A_{11} = \sum_{i=1}^{n} 1 = n, A_{12} = A_{21} \sum_{i=1}^{n} \left(G_{si} + \frac{B_{Si}^2}{G_{si}} \right), \\ &A_{13} = A_{31} = \sum_{i=1}^{n} \frac{1}{G_{Si}}, A_{14} = A_{41} = \sum_{i=1}^{n} \frac{B_{Si}}{G_{Si}}, \\ &A_{15} = \sum_{i=1}^{n} F_i, A_{22} = A_{21} \sum_{i=1}^{n} \left(G_{si} + \frac{B_{Si}^2}{G_{si}} \right), \\ &A_{23} = A_{32} = \sum_{i=1}^{n} \frac{1}{G_{Si}} \left(G_{si} + \frac{B_{Si}^2}{G_{si}} \right), \\ &A_{24} = A_{42} = \sum_{i=1}^{n} \frac{B_{Si}}{G_{Si}} \left(G_{si} + \frac{B_{Si}^2}{G_{si}} \right), \\ &A_{25} = \sum_{i=1}^{n} F_i \left(G_{si} + \frac{B_{Si}^2}{G_{si}} \right), A_{33} = \sum_{i=1}^{n} \frac{1}{G_{Si}^2}, \\ &A_{34} = A_{43} = \sum_{i=1}^{n} \frac{B_{Si}}{G_{Si}^2}, A_{35} = \sum_{i=1}^{n} F_i \frac{1}{G_{Si}}, \\ &A_{44} = \sum_{i=1}^{n} \left(\frac{B_{Si}}{G_{Si}} \right)^2, A_{45} = \sum_{i=1}^{n} F_i \frac{B_{Si}}{G_{Si}}. \end{aligned} \tag{35}$$

T (ratio of the output variable to the input variable) is defined as [31]:

$$T = \frac{\sum_k T_k \Delta_k}{\Delta} \ , \tag{36}$$

where, Δ = 1 - Σ (all individual loop gains) + Σ (loop gain products of all possible combinations of two non-touching loops) - Σ (loop gain products of all possible combinations of three non-touching loops) + …, and Δ_k is the value of Δ not touching the *k*th forward path.

6.3 Y-factor method

NF is a measure of the noise generated by the electronic device. The noise factor (F) is the numerical ratio of NF, where NF is expressed in decibels. The NF for a two-port device can be defined as the ratio of the signal-to-noise power at the input to the ratio of the signal-to-noise power at the output and is given as [19],

$$F = \frac{S_i / N_i}{S_o / N_o} \ , \tag{37}$$

where S_i and S_o are the available signal power at the input and output of a device, whereas N_i and N_o are the available noise power at the input and output of a device, respectively. N_i is referred as kT_oB, where k is the Boltzmann constant, T_o is the temperature, and B is the bandwidth. N_o is related to N_i through

$$N_o = N_a + GN_i \ , \tag{38}$$

where N_a is the noise added by a device during the noise measurement and G is the gain of the device. The most popular method of measuring the NF is based on the *Y*-factor method. Through the *Y*-factor, two states of available noise power are stimulated for the device, which are the ambient thermal noise during the COLD state and the large amount of noise power during the HOT state. The *Y*-factor is described as

$$Y = \frac{N_H}{N_C} \ , \tag{39}$$

where N_H and N_C refer to the available noise power measured at the output of the device during the HOT and COLD states, respectively. Based on the *Y*-factor, NF is obtained through

$$F = \frac{ENR}{Y - 1} \ , \tag{40}$$

where *ENR* is the ENR generated by NFA. NF is usually indicated as the parameter that determines the ability of a receiver to process low-level signals.

Acknowledgements

The authors would like to thank the Universiti Sains Malaysia for the financial support to this work under Short-term Grant No. 304/PCEDEC/60310038. Partial support from CREST Grant No. 304/PELECT/6050262/C121 is also gratefully acknowledged.

References

[1] S. Long, L. Escotte, J. Graffeuil, F. Brasseau, J. L Cazaux, IEEE Transactions on Instrumentation and Measurement, **52**(5), 1606 (2003).

[2] P. Beland, L. Roy, S. Labonte, M. Stubbs, Instrumentation and Measurement Technology Conference IMTC/98. Conference Proceedings. IEEE, May 1998.

[3] Dazhen Gu, David K. Walter, James Randa,

Microwave and Optical Technology Letters, **52**(11), 2600 (2010).
[4] Laurent Escotte, Robert Plana, Jacques Graffeuil, IEEE Transactions on Microwave Theory and Techniques, **41**(3), 382 (1993).
[5] Marco De Dominics, Franco Giannini, Ernesto Limiti, Antonio Serino, Microwave and Optical Letters **44**(6), 565 (2004).
[6] Frederique Giannini, Emmanualle Bourdel, Daniel Pasquet, IEEE Transactions on Instrumentation and Measurement, **57**(2), 261 (2008).
[7] Frederique Giannini, Emmanuelle Bourdel, Daniel Pasquet, in Proc SPIE, 2004, Bellingham, WA.
[8] D. Bourdel, E. Quintanel, S. Ravalet, T. Houssin, P. Pasquet, IEEE Transactions on Microwave Theory and Techniques, **56**(9), 2136 (2008).
[9] D. Pasquet, C. Andrei, D. Lesénéchal, P. Descamps, Physics and International Kharkov Symposium on Engineering of Microwaves, Millimeter and Submillimeter Waves (MSMW), June 21-26, 2010, Kharkiv, Ukraine.
[10] Herbert Hillbrand, Peter H. Russer, IEEE Transactions on Circuits and Systems , **CAS-23**(4), 235 (1976).
[11] Leonid Belostotski, IEEE Transactions on Microwave Theory and Techniques, **59**(4), 877 (2011).
[12] A. Lazaro, L. Pradell, IEEE Electronics Letters, **34**(24), 2352 (1998).
[13] Antonio Lazaro, Lluis Pradell, Juan M. O'Callaghan, IEEE Transaction on Microwave Theory and Techniques, **47(**3), 315 (1999).
[14] Saman Asgaran, Chih-Hung Chen M. Jamal Deen, G. Ali Resvani, Yasmin Kamali, Yukihiro Kiyota, IEEE Journal of Solid-State Circuits, **42**(5), 1034 (2007).
[15] Saman Asgaran, M. Jamal Deen, Chih-Hung Chen, in Radio Frequency Integrated Circuits (RFIC) Symposium, *IEEE,* June 10-13, 2006, San Francisco, CA.
[16] Jianjun Gao, An International Journal of Solid State Electronics, **63**(1), 42 (2011).
[17] Jianjun Gao, Choi Look Law, Hong Wang, S. Aditya, G. Boeck, IEEE Transactions on Microwave Theory and Techniques, **51**(10), 2079 (2003).
[18] Marco De Dominicis, Franco Giannini, Ernesto Limiti, Giovanni Saggio, IEEE Transaction on Instrumentation and Measurement, **51**(3), 560 (2002).
[19] Luuk F. Tiemeijer, Ramon J. Havens, Randy de Kort, Andries J. Scholten, IEEE Transactions on Microwave Theory and Techniques, **53**(9), 2917 (2005).
[20] Cedric Chambon, Laurent Escotte, Sebastien Gribaldo, Olivier Llopis, IEEE Transactions on Microwave Theory and Techniques , **55**(4), 795 (2007).
[21] Leonid Belostotski, James W. Haslett, IEEE Transactions on Microwave Theory and Techniques, **58**(1), 236 (2010).
[22] Sungjae Lee, Kevin J. Webb, Vinayak Tilak, Lester F. Eastman, IEEE Transactions on Microwave Theory and Techniques, **51**(5), 1567 (2003).
[23] Chih-Hung Chen, Ying-Lien Wang, Mohamed H. Bakr, Zheng Zeng, IEEE Transactions on Instrumentation and Measurement, **57**(11), 2462 (2008).
[24] Alper Demir, Ph.D Dissertations, Electrical Engineering and Computer Sciences, University of California, Berkeley, 1997.
[25] Larry Dunleavy. (2011) Understanding Noise Parameter Measurement. [Online]. "http://www.modelithics.com/paper/1437.pdf".
[26] M. Hruskovic, J. Hribik, M. Kostal, M. Groschl, E. Benes, Radioengineering Journal, **4**(2), 18 (1995).
[27] S. Korakkottil Kunhi Mohd, T. Z. A. Zulkifli, O. Sidek, IEICE Electronics Express, **7**(4), 302 (2010).
[28] Agilent Technologies. (1996) S-Parameter Techniques. [Online]. "http://www.sss-mag.com/pdf/hpan95-1.pdf".
[29] Agilent Tehnologies. (2006) Fundamentals of RF and Microwave Noise Figure Measurements. [Online]. "http://cp.literature.agilent.com/litweb/pdf/5952-8255E.pdf."
[30] R. Hu, Tzu-Hsien Sang, IEEE Transactions on Microwave Theory and Techniques, **53**(7), 2398 (2005).
[31] Hewlett-Packard Application Note 95-1. (1967, February) Test and Measurement (Application Note 95-1). [Online]. "http://cp.literature.agilent.com/litweb/pdf/5952-1130.pdf".

*Corresponding author: shukri.mohd@usm.my